Inexpensive Raman Spectrometer for Undergraduate and Graduate Experiments and Research

ARTICLE *in* JOURNAL OF CHEMICAL EDUCATION · FEBRUARY 2010

Impact Factor: 1.11 · DOI: 10.1021/ed800081t

3 AUTHORS, INCLUDING:

Michael Hippler
The University of Sheffield
41 PUBLICATIONS **723** CITATIONS

Cost-Effective Teacher

edited by
Harold H. Harris
University of Missouri—St. Louis
St. Louis, MO 63121

Inexpensive Raman Spectrometer for Undergraduate and Graduate Experiments and Research

Christian Mohr, Claire L. Spencer, and Michael Hippler*
Department of Chemistry, University of Sheffield, Sheffield S3 7HF, United Kingdom
*M.Hippler@sheffield.ac.uk

Spectroscopy is at the heart of physical chemistry. It provides us with tools to determine the structure and dynamics of molecules and molecular association, for analytical applications, and to test theory. Vibrational spectroscopy is particularly relevant, since the pattern of vibrational bands can be analyzed to gain information on the composition and structure of a compound and also provides a characteristic fingerprint for chemical analysis. Vibrational frequency shifts can give information about the local environment of a vibrating group, which can be used to study intermolecular bonding and association.

Raman and IR spectroscopy complement each other. Each method has its own merits, making the method of choice different for different applications. Raman spectroscopy is distinguished by different selection rules, which, for example, lead to greater sensitivity to nonpolar functional groups, and it is also distinguished by minimal sample preparation and nondestructive analysis, ability to easily access low-frequency vibrations, and low sensitivity to water allowing convenient measurements of wet samples or aqueous solutions. It is desirable that students are exposed to both methods in their undergraduate studies. Whereas the theory of Raman spectroscopy is in general treated fairly extensively in the classroom, there is a perceived lack of suitable experiments in the teaching laboratories that provide practical training *(1)*. This issue has been addressed by several recent articles about instructional Raman systems and undergraduate experiments, which are both interesting and relevant *(1−8)*.

We describe the construction and performance of an inexpensive modular Raman spectrometer that has been assembled in the framework of a fourth-year undergraduate project (costs below $5000). The spectrometer is based on a low-power green laser pointer and a compact monochromator. The monochromator is equipped with glass fiber optical connections, a linear detector array, and a USB computer connection that also provides the power supply. The laser source and the Raman spectrometer belong to a low laser safety class that is an important consideration for undergraduate teaching. The setup has the distinct advantage of being modular, compact, and portable; the spectrometer can be operated solely on batteries. With good spectral specifications and performance, the apparatus can be used for research purposes as well. Compared to commercial systems, it is not a "black box" instrument; all components are easily accessible and visible, which makes it ideally suited for lecture and teaching lab demonstrations. We use this spectrometer for various undergraduate and graduate experiments and research, some of which are introduced here.

Setup of the Raman Spectrometer

A schematic of the Raman spectrometer is shown in Figure 1 and details for the main components and photographs of the setup are given as supporting information. The spectrometer uses a green laser pointer to illuminate the sample via a microscope objective. Backscattered Raman radiation is collimated by the same objective, green-laser light is blocked by a filter, and the remaining Raman radiation focused into a glass fiber that is connected to a visible spectrometer with a grating monochromator and linear diode array CCD detector. Signals are transferred via a USB connection to a computer where the signals are processed and displayed.

The components are mounted on a 250 mm × 250 mm × 10 mm aluminum plate with a 50 mm × 50 mm grid of M6 threaded holes for mounting components. The laser source is an inexpensive diode-pumped frequency-doubled green laser pointer emitting less than 4 mW of linearly polarized 532.2 nm radiation (laser class 3R). The laser pointer is battery operated, but to prolong operation time, the battery can be replaced by a dc power supply. The pointer is mounted on a V-clamp to simplify alignment. The green light is turned by 90° by a small mirror and coupled into a microscope objective. The mirror must be as small as possible, so it will not take away too much of the backscattered Raman radiation. For this purpose, we use a glass microscope slide on which we deposited a central 2 mm × 3 mm oval Al film, using a thermal evaporator (Edwards Auto 306; similar evaporators probably available in many university departments). It might also be possible to deposit a reflective silver spot by a chemical reaction (Tollens' reaction). As an alternative, a small 2 mm × 2 mm prism could be used. Another option would be the use a half-reflective beam splitter as mirror, but this would only couple half of the laser intensity into the sample, and it would also take away half of the backscattered Raman light, thus greatly reducing sensitivity. The microscope objective is mounted via an adapter to a post. The achromatic objective (20×, 0.50 NA) has a large clear aperture (8.2 mm) and focuses the green-laser light very tightly at 2 mm distance from the objective front onto the sample.

Liquid samples are contained in a glass vial or in a glass cuvette that is mounted in a thermostatted cuvette holder (retrieved from an unused UV—vis spectrometer). Glass shows almost no fluorescence, whereas plastic cuvettes could not be used owing to strong fluorescence that would mask the weaker Raman scattering. Solid samples can be measured by attaching them to a stand in front of the objective; with the tight focusing

10.1021/ed800081t Published on Web 02/09/2010

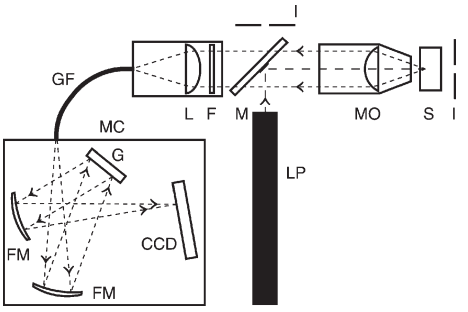

Figure 1. Setup of the Raman spectrometer. LP, laser pointer; M, mirror (glass slide with 2 mm × 3 mm Al spot); MO, microscope objective; S, sample; I, irises; F, filter; L, lens; GF, glass fiber. MC, monochromator with FM: focusing mirrors; G, grating; and CCD, linear charge-coupled device detector array.

spot of the green-laser light, a spatial resolution below 100 μm is achieved.

Raman backscattered light (180° detection geometry) is collimated by the same objective. To block unwanted Rayleigh scattered light from the detector, backscattered light passes through a filter and is then focused with an f = 25.4 mm lens into a fiber patch cable. The filter and the lens are fixed in two lens tubes stacked together and mounted on a cage plate attached to a post. The fiber patch cable is mounted via an adapter to the same cage plate. An inexpensive orange-color glass filter can be used that absorbs light with shorter wavelengths than ca. 560 nm, thus, blocking the 532 nm excitation light and being transparent to red-shifted Stokes scattered light with wavelengths longer than ca. 560 nm. The transmittance cutoff, however, is not very sharp, and Raman light near the cutoff of ca. 560 nm is lost, which prevents the observation of Raman shifts below ca. 1000 cm^{-1}. In addition, blue-shifted anti-Stokes lines below 532 nm can also not be observed with such a glass filter. We thus decided to invest in a high-performance interference notch filter that blocks light around 532 ± 10 nm with a steep transmittance curve allowing the observation of Raman shifts down to ca. 340 cm^{-1} (ca. $500).

The fiber transmits Raman scattered light to a monochromator with a 25 μm entrance slit, 1200 lines/mm holographic grating, and a 3648 pixel diode array CCD detector. The selection of slit width, center wavelength, and grating affords a spectral range of 420−736 nm and a specified resolution of 0.57 at 600 nm. By choosing a different grating, resolution can be increased at the expense of spectral range. For example, a 1800 lines/mm grating would have a resolution of ca. 0.3 at 600 nm with a spectral range of ca. 160 nm; this would be adequate for a Raman spectrometer but would somewhat limit its general use as a visible monochromator as outlined below. After a careful recalibration with Ne and Hg emission lines from a Ne glow lamp (as used in voltage indicators, size NE-2) and a fluorescent light tube (ceiling light), peak positions can be determined with 0.06 nm accuracy (standard deviation of measured lines compared with literature values). Raman spectra thus have an experimental resolution of ca. 20 cm^{-1} and accuracy of 2 cm^{-1}, which should be adequate for most measurements in the condensed phase.

Most of the noise in a spectrum recorded by the CCD array arises from different dark currents of the different pixels. This systematic noise can almost completely be canceled by subtracting a stored dark spectrum recorded with the laser switched off. Remaining statistical noise can be minimized by increasing the integration time during exposure of the CCD array to achieve high signal levels and by accumulating and averaging several spectra. Typical integration times range from 100 ms for the strong Raman scatterer benzene and more than 10 s for the much weaker scatterer water. Spectral data are transferred via an USB connection to a computer. This connection also powers the spectrometer. Spectra are manipulated and displayed with Ocean Optics software "SpectraSuite". Liquid benzene kept in a sealed glass vial is suitable for the initial optical alignment. With short integration times, optical components can be aligned by optimizing Raman signals without noticeable delay. After optimization, the laser-beam path is defined by two irises, and only minor readjustments of the laser pointer are occasionally necessary. Note that since the laser light is linearly polarized, the Raman spectrometer could also be used for polarization-sensitive measurements (e.g., depolarization ratios) if appropriate polarizers are used.

Hazards

With 4mW visible output, the laser pointer is a class 3R laser device, that is, safe if handled carefully. We enclosed the region between the microscope objective and the glass fiber connection with panels made of gray, transparent glass (on the top) and black card (on the sides) with an opening on one side to receive the laser pointer. The region where the laser beam is collimated is thus restricted from direct viewing, but alignment of the laser pointer is still possible. Light exits this enclosure at the objective where it is highly divergent after the sharp focus. Since the beam is diverging and direct viewing of the collimated beam is restricted, the apparatus is class 2M, that is, considered safe for accidental viewing during normal use. In addition, the instrument has a cover of black cardboard, which is closed during measurements to prevent stray light from entering the spectrometer, and also serves to protect the user from any stray laser light.

Application Examples

Benzene

A Raman spectrum of liquid benzene to demonstrate the performance of the instrument is shown in Figure 2. Dominant bands are the symmetric CH-stretching vibration around 3060 cm^{-1} and the symmetric CC-ring-breathing vibration around 990 cm^{-1}. This shows the complementary nature of Raman and IR spectroscopy, where these vibrations are IR-inactive, an example of the mutual exclusion rule of centrosymmetric molecules. In Figure 2, a weak background caused by autofluorescence is visible that disappears below ca. 340 cm^{-1} because of the cutoff of the notch filter. The notch filter is efficient in rejecting most of the Rayleigh scattered light from the green laser (remaining peak marked by an asterisk in Figure 2). Below 525 nm, weaker anti-Stokes transitions can be seen. By comparing intensities of Stokes−anti-Stokes counterparts, the temperature of the sample can be determined by application of the Boltzmann distribution law. Measuring peak intensities of Stokes−anti-Stokes bands as a function of temperature, the Boltzmann distribution law can be experimentally verified *(2)*.

Demonstrations and Experiments

Because the spectrometer is modular and portable, it can be used in the classroom for practical lecture demonstrations to

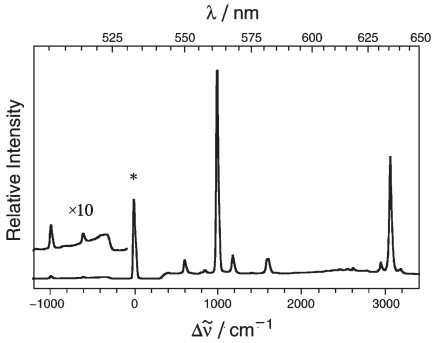

Figure 2. Raman spectrum of liquid benzene at room temperature (5 s integration time, average of 100 spectra). The peak from the Rayleigh scattered light is marked by an asterisk.

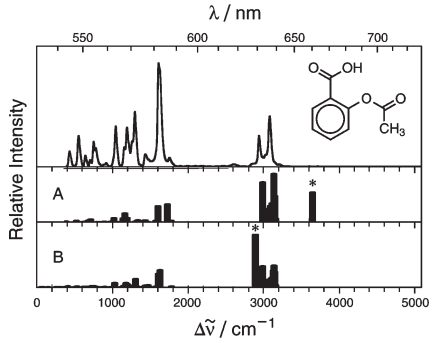

Figure 3. Raman spectrum of a aspirin tablet (upper plot; 3 s integration time, average of 200 spectra) in comparison with calculated spectra (Raman scattering activities) (A) monomer and (B) dimer (DFT, B3LYP/6-31G(d,p)++, scaling factor 0.978). A strong OH-stretching vibration is marked by an asterisk in (A). Raman-active symmetric OH-stretching vibration is marked by asterisk in (B).

reinforce the theory of vibrational and Raman spectroscopy, laser techniques, and UV−vis spectroscopy. Owing to the modular approach, the monochromator can be used on its own. By pointing the fiber probe to different light sources, the spectrum of a black-body radiator (tungsten light bulb) can be shown in a physical chemistry lecture or Ne emission lines from a Neon glow lamp and Hg emission lines from a fluorescent light tube (ceiling light) in lectures on atomic spectroscopy (there are some prominent visible Hg lines; most of the Hg emission occurs in the UV, however, and is converted into visible light by the phosphor coating of the lamp). In a third-year practical project, a simple visible spectrometer is assembled on a bench, consisting of the tungsten bulb of a desk lamp as light source, a sealed glass cell containing iodine vapor as a sample, and the monochromator to record the visible absorption spectrum of iodine vapor. In the project, the spectrum is analyzed to demonstrate the Franck−Condon principle and hot-band transitions and to extract dissociation energies of the ground and electronically excited state *(9)*.

Raman spectroscopy is ideally suited for analytical applications without destroying or damaging the sample. Because of its backscattering geometry, it can be used for liquid and solid samples. In fourth-year undergraduate experiments, the Raman spectrometer has been employed to determine the authenticity of gemstones (e.g., distinguishing diamonds from its simulant cubic Zirconia; refs *1* and *2*), to analyze the shift of XH-stretching bands on deuteration of a compound, for example, water or chloroform (to reinforce the theory of vibrational spectroscopy) *(2)*, or to determine the alcohol content of some beverages. Since similar experiments have been described before *(1, 2, 5, 7, 8)*, we do not provide further detail, but introduce two selected applications.

Aspirin Tablets

Spectra of solid acetylsalicylic acid (aspirin) tablets have been recorded and analyzed to demonstrate the use of Raman spectroscopy in nondestructive chemical analysis, drug authentication in forensic chemistry, and in a more fundamental study of molecular association by hydrogen bonding. Aspirin has characteristic Raman and IR vibrational spectra. While IR spectra of aspirin are usually taken in a KBr matrix requiring involved sample preparation, Raman spectra of solid tablets or of the powder contained in a glass vial can be directly recorded in the backscattering geometry described. Tablets of pure aspirin (Fluka, purum) and aspirin synthesized from the reaction of salicylic acid and acetic anhydride (a typical undergraduate experiment) have been produced with a pellet press. These tablets have been measured and compared with commercial tablets containing aspirin as the main ingredient.

The Raman spectrum of lab-synthesized aspirin as a representative example is shown in Figure 3. The dominating feature is a partly resolved double peak at 1606 and 1622 cm^{-1}, which is assigned as a symmetric aromatic ring CC-stretching vibration and the CO-stretching vibration of the carboxy group, respectively. In the wing of this feature at 1752 cm^{-1}, the much weaker CO-stretching vibration of the ester group is apparent. Below 1500 cm^{-1}, there are several medium-strong peaks, the strongest one being an OH-bending vibration at 1293 cm^{-1}. Around 3000 cm^{-1}, several medium-strong CH-stretching vibrations on saturated and unsaturated carbons are observed (for a full list of assignments, see ref *10*). In a typical analytical application, such a characteristic spectrum can be used as a fingerprint to identify and determine the purity of a compound, for example, by comparison with spectra from a database. We are currently planning an undergraduate experiment where the aspirin content of commercial pain relief tablets is quantitatively determined and other constituents identified by Raman spectroscopy (see ref *11* for a similar application on the analysis of aspirin−maize starch tablets).

In combination with theoretical calculations, spectroscopy can provide detailed insight into molecular properties. We performed some simple ab initio quantum-chemical calculations on Raman vibrational spectra that are suitable for undergraduate projects, using a PC with the freely available GAMESS (US) and PC-GAMESS/FIREFLY quantum chemistry packages *(12, 13)*. In these calculations, we employed split valence 6-31G or 6-311G basis functions with added polarization functions (d,p) and diffuse functions (++). To include electron correlation, second-order Møller−Plesset perturbation theory (MP2) or density-functional theory (DFT) with the B3LYP functional has been used. In most cases, satisfactory agreement between predicted and observed spectrum is obtained (see also refs *6* and *7*). It is thus interesting to note that this is not the case for aspirin: the B3LYP/6-31G-(d,p)++ calculations predict, for example, a strong, prominent OH-stretching vibration around 3650 cm^{-1} (frequency scaled by 0.978). This peak is marked by an asterisk in the calculated

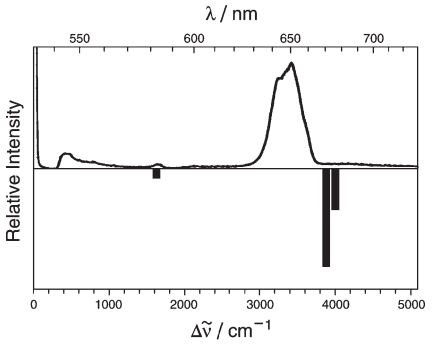

Figure 4. Raman spectrum of liquid water at room temperature (upper plot; 10 s integration time, average of 200 spectra), in comparison with a calculated spectrum (vertical bars are Raman scattering activities; MP2/6-311G(d,p)++, scaling factor 0.95).

spectrum of Figure 3A, but it is not apparent in the experimental spectrum. These calculations do not take into the strongly associated cyclic hydrogen bonds in the solid matrix:

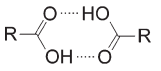

Because of this interaction, the OH-stretching band is broadened and shifted toward lower wavenumbers (often called a "red shift"; although this is standard terminology, it appears to us that red shift is a misnomer since there is no red or blue spectral region in the IR, and a shift toward the red or blue would, strictly speaking, always imply a shift toward the visible region, that is, toward higher wavenumbers). We performed a more detailed calculation of aspirin dimer (similar to ref *10*) that resolves this discrepancy. Starting from an initial geometry from the crystal structure, the ab initio calculation converges to a cyclic hydrogen-bonded dimer of C_i symmetry in a "cis" configuration (OH and ester group on the same side of the molecule). In the calculation, the Raman-active symmetric OH-stretching vibration shifts into the region of the CH-stretching vibrations at around 2900 cm^{-1} (Figure 3B, peak marked by asterisk). Further calculations predict that the band is, in addition, considerably broadened and mixed with CH-stretching vibrations *(10)*. Qualitative agreement between calculations and experiment is observed confirming the presence of hydrogen bonding in solid aspirin.

Liquid Water

In a second application, Raman spectra of liquid water have been recorded. These spectra are complex owing to the formation of an extended hydrogen-bonded network. The analysis and interpretation of spectra is of great interest and relevance, since most of the anomalies of water are attributed to the structure of the network and its rearrangement processes. Experimental studies include spectroscopy at different temperatures, pressures, or in the presence of various solutes, and results are most often interpreted on the basis of various theoretical calculations or models (see, e.g., refs *14*–*17*). Amazingly there still seems to be no consensus on how to interpret liquid water spectra. This application thus provides the opportunity to introduce students to a relevant topic of current research and debate.

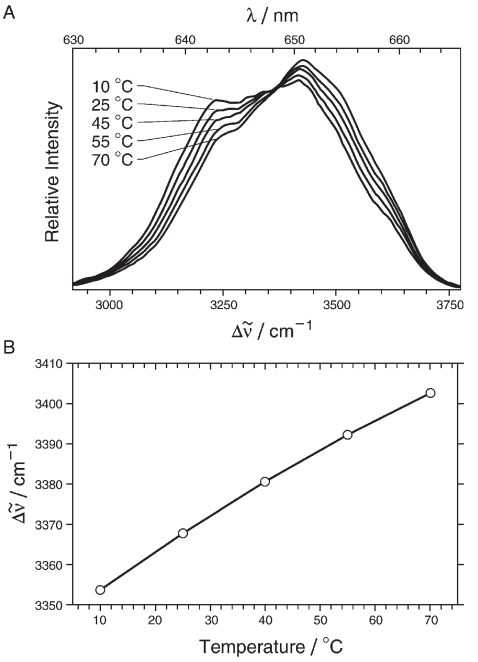

Figure 5. (A) Raman spectra of the OH-stretching region of liquid water at different temperatures (10 s integration time, average of 200 spectra; spectra normalized to same area). (B) Plot shows how the center-of-gravity $\Delta\tilde{\nu}$ of the Raman band changes with temperature.

Although water is a weak Raman scatterer, good spectra are obtained if a suitably long signal integration time is chosen (Figure 4). Isolated H_2O has three normal-mode vibrations: the asymmetric OH-stretching vibration ν_3 and the symmetric stretching ν_1 near 4000 cm^{-1} and the bending vibration ν_2 around 1600 cm^{-1} (see Figure 4 for the ab initio prediction of the Raman spectrum). The observed Raman spectrum of the liquid, however, is different and more complex: the bending vibration is observed at 1645 cm^{-1}, close to the position predicted for isolated H_2O, but the stretching vibrations are significantly shifted toward lower wavenumbers and form a broad, structured feature with a full width at half-maximum ca. 450 cm^{-1}. This broadening is genuine and not an artifact owing to insufficient experimental resolution (given as ca. 20 cm^{-1} and verified on the sharp features of the benzene spectrum, see Figure 2).

The dominant OH-stretching feature around 3000−3700 cm^{-1} is shown in Figure 5 in more detail. The vibrational frequency shift and broadening is caused by hydrogen bonding, where the extent of the shift is given by different hydrogen-bonding situations, dependent on the number and type of hydrogen bonds (single, bifurcated, or trifurcated), the hydrogen-bond length, and bending angle. As a rule, the frequency shift toward lower wavenumbers increases with increasing hydrogen-bond strength. In the liquid, hydrogen bonds are formed and broken within picoseconds, and there is a dynamic equilibrium of different environments. With increasing temperature, water molecules experience, on average, weaker hydrogen bonding, and the frequency shift should be less pronounced. This is observed in our temperature-dependent spectra (see Figure 5), where the center-of-gravity of the feature (defined as the frequency where the integrated intensity is at its half value) changes from 3352 cm^{-1} at 10 °C (stronger hydrogen bonds) to 3401 cm^{-1} at 70 °C (weaker hydrogen bonds).

Whereas there seems to be a consensus on the general appearance of the OH-stretching feature as outlined above, there is still much debate on the assignment of its apparent structure. The structure has been analyzed by decomposition into various Gaussian-shaped components, but there is no agreement on the number of components (ranging from 3 to 5). There are at least two different explanations for the physical origin of the components. In one explanation, the structure is assigned to the frequency-shifted symmetric and asymmetric stretching vibrations derived from the normal modes of the isolated molecule, where the symmetric stretching mode ν_1 is in addition in a strong anharmonic vibrational resonance ("Fermi-resonance") with the bending overtone $2\nu_2$ *(14, 15)*. This resonance is already clearly apparent in isolated, gas-phase H_2O but even more pronounced in the liquid, where the frequency shift tunes ν_1 and $2\nu_2$ into closer resonance. In an alternative, opposing explanation, the structure is assigned to originate from different distinct hydrogen-bonded−nonhydrogen-bonded environments in thermal equilibrium, for example, corresponding to water with three or four hydrogen bonds *(16, 17)*. This assignment seems to be corroborated by the observation of isosbestic points in temperature-dependent spectra *(16)* and by a van't Hoff plot of the intensities of components that gives an enthalpy difference corresponding to the breaking of one hydrogen bond *(17)*. As mentioned before, however, a conclusive assignment is still subject of ongoing research.

Conclusions

We have described the setup of a cost-effective, small, portable, and modular Raman spectrometer suitable for undergraduate and graduate experiments and research and characterized its performance. The spectrometer has been constructed in the framework of a fourth-year project. The instrument is versatile and has many applications in undergraduate teaching, including analytical and forensic chemistry and spectroscopy. Owing to its good specifications, it is also used for more fundamental research, for example, concerning molecular association by hydrogen bonding in solid acetylsalicylic acid or liquid water. These advanced applications may provide an opportunity to introduce students to relevant topics of current research in spectroscopy.

Acknowledgment

We are grateful to Georg Seyfang (ETH Zürich) for helpful discussions on the instrument design. The setup of the spectrometer was supported by a Royal Society Equipment grant.

Literature Cited

1. Pharr, C.; Neff, H.; Sullivan, A.; Tiegs, S. Raman Spectroscopy in Education. In *Handbook of Vibrational Spectroscopy*; Chalmers, J. M., Griffiths, P. R., Eds.; John Wiley and Sons, Ltd.: New York, 2002; Vol. 4, pp 3217−3226.
2. Galloway, D. B.; Ciolkowski, E. L.; Dallinger, R. J. *J. Chem. Educ.* **1992**, *69*, 79.
3. Voor, R.; Chow, L.; Schulte, A. *Am. J. Phys.* **1994**, *62*, 429.
4. Fitzwater, D. A.; Thomasson, K. A.; Glinski, R. J. *J. Chem. Educ.* **1995**, *72*, 187.
5. Aponick, A.; Marchozzi, E.; Johnston, C.; Wigal, C. T. *J. Chem. Educ.* **1998**, *75*, 465.
6. Comstock, M. G.; Gray, J. A. *J. Chem. Educ.* **1999**, *76*, 1272.
7. McClain, B. L.; Clark, S. M.; Gabriel, R. L.; Ben-Amotz, D. *J. Chem. Educ.* **2000**, *77*, 654.
8. Vickers, T. J.; Pecha, J.; Mann, C. K. *J. Chem. Educ.* **2001**, *78*, 1674.
9. McNaught, I. J. *J. Chem. Educ.* **1980**, *57*, 101.
10. Boczar, M.; Wójcik, M. J.; Szczeponek, K.; Jamróz, D.; Zięba, A.; Kawałek, B. *Chem. Phys.* **2003**, *286*, 63.
11. Kontoyannis, C. G.; Orkoula, M. *Talanta* **1994**, *41*, 1981.
12. Schmidt, M. W.; Baldridge, K. K.; Boatz, J. A.; Elbert, S. T.; Gordon, M. S.; Jensen, J. H.; Koseki, S.; Matsunaga, N.; Nguyen, K. A.; Su, S. J.; Windus, T. L.; Dupuis, M.; Montgomery, J. A. *J. Comput. Chem.* 1993, *14*, 1347; http://www.msg.chem.iastate.edu/gamess (accessed Dec 2009).
13. Granovsky, A. A. *PC GAMESS/Firefly version 7.1.C*, http://classic.chem.msu.su/gran/gamess/index.html (accessed Dec 2009).
14. Weston, R. E. *Spectrochim. Acta* **1962**, *18*, 1257.
15. Sceats, M. G.; Stavola, M.; Rice, S. A. *J. Chem. Phys.* **1979**, *71*, 983.
16. Walrafen, G. E.; Hokmabadi, M. S.; Yang, W.-H. *J. Chem. Phys.* **1986**, *85*, 6964.
17. Carey, D. M.; Korenowski, G. M. *J. Chem. Phys.* **1998**, *108*, 2669.

Supporting Information Available

Details for the main components and photographs of the Raman spectrometer. This material is available via the Internet at http://pubs.acs.org.

